AGU PUBLICATIONS

Geophysical Research Letters

RESEARCH LETTER

10.1002/2014GL060826

Key Points:
- Arctic spring atmosphere can be used for prediction of September sea ice
- Simple models using spring atmospheric predictors provide high predictive skills
- The skills of these simple models are similar to those of complex models

Correspondence to:
M.-L. Kapsch,
marie@misu.su.se

Citation:
Kapsch, M.-L., R. G. Graversen, T. Economou, and M. Tjernström (2014), The importance of spring atmospheric conditions for predictions of the Arctic summer sea ice extent, *Geophys. Res. Lett.*, *41*, 5288–5296, doi:10.1002/2014GL060826.

Received 7 JUN 2014
Accepted 14 JUL 2014
Accepted article online 17 JUL 2014
Published online 28 JUL 2014

The importance of spring atmospheric conditions for predictions of the Arctic summer sea ice extent

Marie-Luise Kapsch[1,2], Rune G. Graversen[1,2], Theodoros Economou[3], and Michael Tjernström[1,2]

[1]Department of Meteorology, Stockholm University, Stockholm, Sweden, [2]Bolin Center for Climate Research, Stockholm University, Stockholm, Sweden, [3]College of Engineering, Mathematics and Physical Sciences, University of Exeter, Exeter, UK

Abstract Recent studies have shown that atmospheric processes in spring play an important role for the initiation of the summer ice melt and therefore may strongly influence the September sea ice concentration (SSIC). Here a simple statistical regression model based on only atmospheric spring parameters is applied in order to predict the SSIC over the major part of the Arctic Ocean. By using spring anomalies of downwelling longwave radiation or atmospheric water vapor as predictor variables, correlation coefficients between observed and predicted SSIC of up to 0.5 are found. These skills of seasonal SSIC predictions are similar to those obtained using more complex dynamical forecast systems, despite the fact that the simple model applied here takes neither information of the sea ice state, oceanic conditions nor feedback mechanisms during summer into account. The results indicate that a realistic representation of spring atmospheric conditions in the prediction system plays an important role for the predictive skills of a model system.

1. Introduction

The reduction and thinning of the Arctic summer sea ice cover is one of the most distinct signals of the ongoing climate change [*Holland and Bitz*, 2003; *Serreze and Barry*, 2011]. Besides this long-term trend, the Arctic sea ice shows large year-to-year variability [*Serreze et al.*, 2007]; e.g., in 2013 the September sea ice extent was found to be around 30% higher than in September 2012. The trend in the September sea ice extent can to a large extent be attributed to long-term changes in the greenhouse gas forcing [*Min et al.*, 2008; *Intergovernmental Panel on Climate Change*, 2013], while atmospheric processes on shorter time scales are suggested to be an important driver for the interannual sea ice variability [*Wang et al.*, 2009; *Eastman and Warren*, 2010; *Graversen et al.*, 2011; *Wu et al.*, 2012; *Ogi and Wallace*, 2012; *Sedlar and Devasthale*, 2012; *Kapsch et al.*, 2013].

Seasonal forecasting of this Arctic sea ice variability is of particular interest for stakeholders that coordinate marine access of the Arctic Ocean [*Arctic Climate Impact Assessment*, 2004; *Eicken*, 2013]. Thus, a variety of approaches have been used to predict the September sea ice extent [cf. *J. Stroeve et al.*, 2014]. Using statistical multiple regression models based on the sea ice state, such as the multiyear ice concentration or sea ice concentration in March, *Drobot* [2007] showed that skillful predictions of the September ice extent for almost all Arctic regions can be achieved. However, most of the current seasonal forecast systems exhibit no significant forecast skills for the September ice variability for lead times of more than a few months: *Lindsay et al.* [2008] found statistically significant forecast skills for lead times of less than 3 months only, using an empirical model based on historical atmosphere, ocean, and ice data; *Sigmond et al.* [2013] and *Wang et al.* [2013] showed that even with a more complex model setup, including dynamics and interactions of atmosphere, sea ice and ocean, prediction skills for the September sea ice cover (SSIC) longer than 3 months are not significant. Recently, *Chevallier et al.* [2013] achieved significant predictive skills for predictions of September Arctic sea ice extent initialized on May 1, thus a lead time of 4 months, using a coupled atmosphere-ocean general circulation model and focusing particularly on a more realistic initialization of each model component.

Here linear regression models based on atmospheric variables in spring (April/May) are designed for predicting the SSIC. The selection of variables is based on the findings by *Kapsch et al.* [2013], showing that

specifically the amount of downwelling longwave radiation in spring, associated with positive humidity and cloud anomalies, plays a significant role for the sea ice cover of the following summer. Thus, we use the atmospheric variables discussed in this study as predictor variables in the model specification. We provide a quantification of the model skills and a discussion of the importance of these atmospheric variables for skillful SSIC predictions.

2. Data and Methods

2.1. Data and Data Preprocessing

The atmospheric variables used as predictors in our model setup are the net shortwave radiation (SWN), net longwave radiation plus turbulent fluxes (sensible and latent; LWNT), the downwelling shortwave (SWD) and longwave radiation (LWD), the vertical integrated water vapor (VIWV) and cloud water (VICW), and the divergence of latent (DivQ) and dry-static energy (DivD). All data are extracted from ERA-Interim reanalysis from the European Centre for Medium-Range Weather Forecast (ECMWF) [*Dee and Uppala*, 2009; *Dee et al.*, 2011], which is one of the best among the data sets representing Arctic climate [e.g., *Lindsay et al.*, 2014; *Zygmuntowska et al.*, 2012]. The data have a $0.5° \times 0.5°$ horizontal resolution and are available for the period 1979–2013. For the radiative and turbulent fluxes 24 h forecast accumulations, initiated at 00 UTC, are used. For all other variables, 6-hourly analyses are averaged to daily values. The meridional energy transport is estimated at a 6 h resolution on model hybrid levels and vertically integrated from the top to the bottom of the atmosphere. A barotropic mass transport correction is applied [*Trenberth*, 1991; *Graversen et al.*, 2007].

All data are detrended, since the focus here is on the year-to-year variability of the SSIC rather than the long-term trend. A second-order polynomial trend, estimated using a least squares fit over 1979–2013, was subtracted from all data. A second-order trend is chosen in order to take the accelerated trend of the SSIC in the second part of the observation period (late 1990s and onward) into account. Note that the results presented in section 3.1 are to some extent sensitive to the order of the subtracted trend. However, the main conclusion is independent of the chosen trend. Further, all variables used in this study are averaged over April and May and the area 70°N to 85°N and 105°E to 20°W, including (from west to east) the Laptev, East Siberian, Chukchi and Beaufort Sea, the Canadian Basin, and the area north of Greenland. In this area the SSIC was found to be significantly related to spring atmospheric conditions that alter the timing of the initiation and the strength of the ice melt in spring [*Kapsch et al.*, 2013]. Note that the study area does not comprise the Greenland, Norwegian, Kara, and Barents Seas, where the ice variability is likely dominated by the inflow of warm Atlantic water [*Smedsrud et al.*, 2013]. However, the area includes the major part of the Arctic, including the Arctic Ocean north of Siberia, where ice variability is large [*Cavalieri and Parkinson*, 2012].

2.2. Statistical Model Development

In order to investigate the predictive potential of the spring atmospheric conditions on the SSIC, a variety of linear regression models (LRMs), based on simple and multiple linear regression techniques, were developed. Each simple LRM uses one of the atmospheric variables mentioned in section 2.1 as a predictor variable. The LRM provides a SSIC prediction based on

$$y_i = \beta_0 + \beta_1 x_{i,1} + \epsilon_i. \tag{1}$$

Here y_i is the SSIC (also referred to as predictand) for each year i, with $i = 1, ..., n$, where n is the number of years used to fit the model; $x_{i,1}$ is the predictor (spring anomaly of an atmospheric variable); β_0 and β_1 are linear regression coefficients; and ϵ_i, for $i = 1, ..., n$, are error terms (also referred to as residuals) that account for the deviation of the SSIC observations from $\beta_0 + \beta_1 x_{i,1}$ [*Draper and Smith*, 1998]. The residuals are assumed to be normally distributed. Thus, equation (1) can more formally be expressed as

$$y_i \sim N\left(\beta_0 + \beta_1 x_{i,1}, \sigma^2\right), \tag{2}$$

where $N(x, \sigma^2)$ is a normal distribution with mean x and variance σ^2 (residual variance). Prediction intervals expressing the uncertainty around the predicted y_i are calculated. The prediction intervals incorporate both the epistemic uncertainty, due to the estimation of the model parameters, and the "natural" variability of y_i captured by σ^2 [*Wilks*, 2006]. Here such intervals are used (Figure 2) to reflect all the uncertainty in the predicted values of the SSIC.

To examine whether combinations of predictor variables would lead to an increase in the predictive skills, a multiple linear regression approach is applied using either two or four predictor variables as well as their interactions. For example, in the case of two variables, the model becomes

$$y_i = \beta_0 + \beta_1 x_{i,1} + \beta_2 x_{i,2} + \beta_3 (x_{i,1} \times x_{i,2}) + \epsilon_i, \quad (3)$$

where $x_{i,1}$ and $x_{i,2}$ are the predictor variables and $(x_{i,1} \times x_{i,2})$ their interaction, while $\beta_0, \ldots, \beta_3$ are the linear regression coefficients. By including the interaction, defined as the product $(x_1 \times x_2)$, an additional effect associated with the mutual dependence of x_1 and x_2 is taken into account.

2.3. Model Evaluation

To assess predictive skills, 80% of the data are randomly selected and used to fit the LRMs. The remaining 20% are used for the SSIC predictions. These 80% and 20% of the data are hereafter referred to as fitting and prediction period, respectively. The mean absolute error (MAE), the mean-squared error (MSE), and the Pearson-correlation coefficient [*Wilks*, 2006] between observed and predicted SSIC are calculated for both the fitting and the prediction period [see also *Breiman and Spector*, 1992]. Note that the MSE is more sensitive to outliers than the MAE. Thus, the MAE is used to evaluate the prediction in general, while the MSE is used to evaluate the prediction of extremes.

To evaluate whether the models have real predictive skills, the LRMs are compared to random chance (RC) and climatology persistence (CP) models [*Drobot et al.*, 2006; *Jolliffe and Stephenson*, 2012]. The CP models are simply the mean SSIC for the fitting period. The RC models are constructed by randomly shuffling the predictor variable over the entire time period, so that the physical relationship between the predictor variable and the SSIC is suppressed. If MAE or MSE values for a given LRM are lower than those for the corresponding RC and CP models the LRM exhibits real predictive skill.

In order to thoroughly test the significance of the results a Monte Carlo method is applied. To get robust error estimates, we randomize the selection of the fitting period and repeat this selection 1000 times. The skill measures are calculated for each iteration and finally averaged. In addition, a Monte Carlo approach is applied on the shuffling of the input variables for the RC models. For each of the randomly selected fitting periods, the shuffling of the predictor variable is repeated 500 times. MAE, MSE, and the Pearson correlation coefficient are averaged over all iterations.

3. Results

Does a simple model that only uses one or two atmospheric variables during spring provide similar predictive skills than more complex model systems? Here we attempt to answer this question using a simple linear regression technique, neglecting other factors such as sea ice preconditioning in form of, e.g., sea ice concentration or thickness changes [*Chevallier and Salas-Mélia*, 2012], dynamical sea ice export due to wind forcing in connection with atmospheric circulation patterns [*Ogi and Wallace*, 2012], oceanic conditions [*Maksimovich and Vihma*, 2012], and physical processes, including sea ice feedback processes, that take place during the entire summer season [e.g., *Kay et al.*, 2008].

3.1. Prediction of SSIC

During the fitting period most of the LRMs based on simple linear regression outperform RC and CP models (Figure 1a). Hence, there is a significant statistical relationship between the predictor variables used in the LRMs and the SSIC. The best fitting models according to the MAE error estimates are those based on downwelling longwave radiation (LWD), vertically integrated water vapor (VIWV), net longwave radiation plus turbulent fluxes (LWNT), or shortwave down radiation (SWD). Their similar performance in the fitting period is due to the physical connection between those variables, implying that they are dependent on each other. For instance downwelling longwave radiation and water vapor or clouds are highly correlated ($r = 0.92$ and $r = 0.69$, respectively). In years with a strong greenhouse effect, meaning that more water vapor and clouds are present in the atmospheric column, more longwave radiation is emitted toward the surface. However, clouds also reflect incoming shortwave radiation back to space due to their high albedo. Thus, in years where the downwelling longwave radiation is anomalously high the amount of shortwave radiation reaching the surface is small and vice versa (Figure 2d; $r = -0.79$). The high anticorrelation between the two variables results in similar MAEs of the corresponding simple LRMs based on downwelling longwave or shortwave radiation (Figures 1a and 2c), only the regression coefficients of these two LRMs have opposite signs.

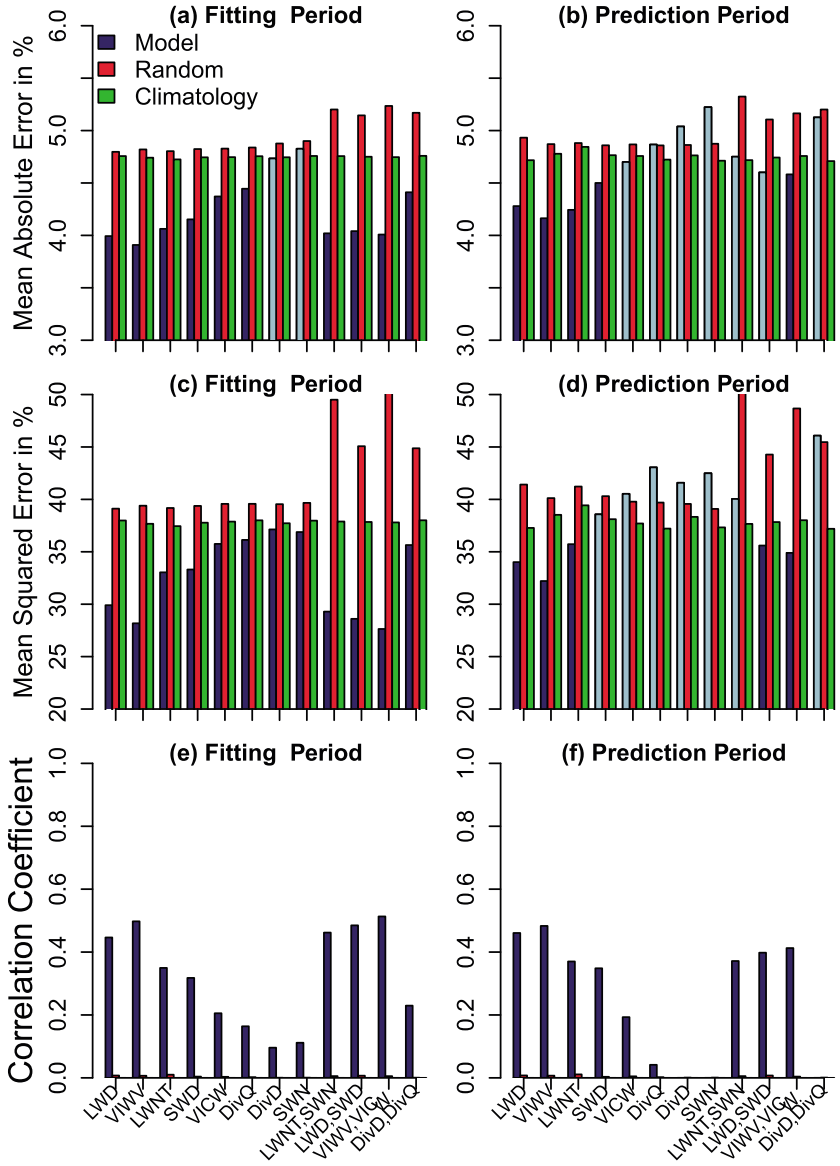

Figure 1. Prediction skills for the 12 simple and multiple linear regression models (see section 2.1 for abbreviations) used to predict September sea ice concentration anomalies; (a and b) the mean absolute error for the fitting period (80% of the data) and the prediction period (20% of the data), respectively. (c and d) The corresponding mean-squared errors are displayed and (e and f) the correlation coefficients between modeled and observed (ERA-Interim) September ice concentration anomalies are shown. Blue, red, and green bars indicate error estimates for the reference LRMs, the random chance, and the climatological models, respectively (see text for further details). Note, most random chance and climatology models have a correlation coefficient close to zero. Light blue colors mark LRM error estimates that are not significantly greater/lower than those of the random chance (RC) or climatology persistence (CP) models (one-tailed Kolmogorov-Smirnov test, $p < 0.05$).

Since downwelling longwave and shortwave radiation are both dependent on the amount of clouds and water vapor, the MAEs for the LRMs using water vapor or cloud water are similar to that of the downwelling radiation-based LRMs (Figure 1a). This result is consistent with *Kapsch et al.* [2013], who found that in years with an enhanced downwelling longwave radiation in spring less SSIC was observed. Note that the LRM based on latent energy convergence also outperforms RC and CP models for the fitting period. The latent energy convergence is highly correlated with the amount of cloud water ($r = 0.93$), indicating that the transport of moisture into the Arctic domain leads to an increased likelihood for cloud formation.

For the prediction period (Figure 1b) the simple LRMs using downwelling longwave radiation, water vapor, longwave net radiation, or shortwave down radiation outperform the RC and CP models. This indicates that

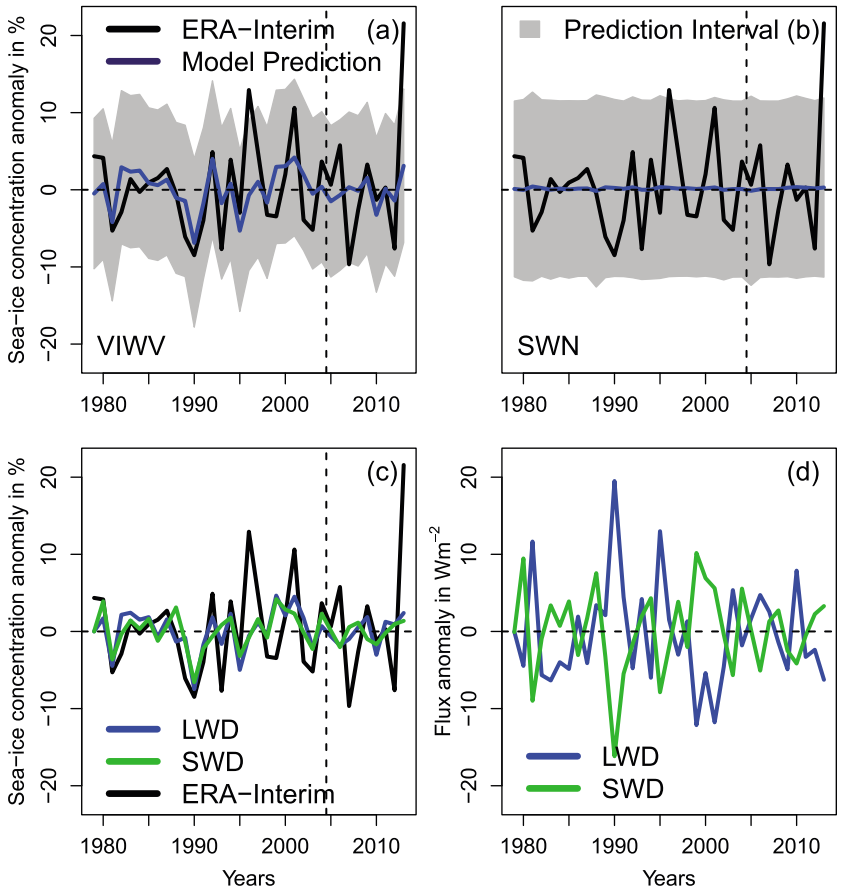

Figure 2. The observed (ERA-Interim) and predicted September sea ice concentration anomalies as a function of year for the models with (a) vertical integrated water vapor (VIWV) and (b) shortwave net radiation (SWN) as predictor variables are shown. Gray shading indicates the prediction interval. (c) The SSIC prediction based on downwelling longwave (LWD) and downwelling shortwave radiation (SWD) anomalies and (d) the corresponding LWD and SWD flux anomalies in spring (April/May). Dashed vertical lines in Figures 2a–2c are separating the fitting (1979–2006) and prediction period (2007–2013).

the LRMs based on each of those four variables exhibit real skills for the SSIC prediction. The LRMs using surface net shortwave radiation or the divergence of dry-static energy show significantly larger errors than the RC and CP models.

The good performance of the LRMs using downwelling longwave radiation and water vapor as predictors is partly a consequence of the initiation of the surface melt by positive downwelling longwave anomalies. In years with an enhanced greenhouse effect in spring, due to more water vapor and clouds in the atmosphere, more longwave radiation is emitted toward the surface. This energy surplus at the surface causes an early melt onset and melt ponds as well as small areas of open water start to form. This is reflected in a strong anticorrelation between spring downwelling longwave radiation and the sea ice concentration in the end of the spring (late May; Figure 3). Due to the appearance of melt ponds and open water, the surface albedo decreases early in the season, and more net shortwave radiation is absorbed by the surface throughout the rest of the melt season (ice-albedo effect). Hence, spring downwelling longwave radiation and net shortwave radiation are significantly correlated throughout the summer (Figure 3). The results indicate that enhanced downwelling longwave radiation in spring leads to an earlier onset of ice melt which in turn initiates the ice-albedo feedback that causes additional melt during the summer. To further investigate the physical connection between the spring downwelling longwave radiation and the melt onset a simple LRM using the sea ice concentration as predictor variable was developed. The model shows similar predictive skills (MAE = 4.7; not shown) compared to those models using downwelling longwave radiation or water vapor as predictor (MAE = 4.3 and MAE = 4.2, respectively; cf. Figure 1b), though the MAEs of the two latter models are significantly lower than the LRM based on the sea ice concentration. This is consistent

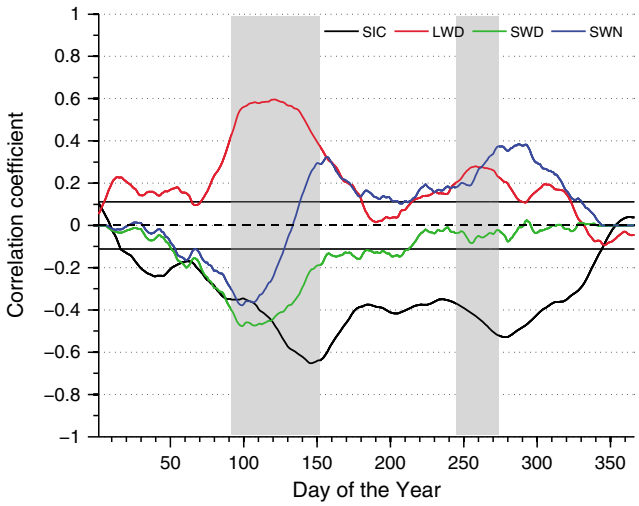

Figure 3. Correlation coefficients between anomalies of downwelling longwave radiation averaged over April/May and sea ice concentration (black), downwelling longwave (red), downwelling shortwave (green), and net shortwave radiation anomalies (blue) as function of time. Black horizontal lines display the significance level of the correlation coefficients (two-tailed t test, $p < 0.05$). Gray-shaded areas mark the time periods April to May and September, respectively. Daily data are used and a 30 day running mean filter is applied to all time series.

with the findings that sea ice melt is likely initiated by the longwave radiation, as shown by the autocorrelations of downwelling longwave radiation having an earlier maximum than the correlations with the sea ice concentration (Figure 3).

The reason for the poor performance of the LRM using the net shortwave radiation can likely be explained by the following physical mechanism: The surface net shortwave radiation is linearly dependent on the amount of downwelling shortwave radiation and the surface albedo. In a spring Arctic atmosphere with only a few clouds and little water vapor, and hence a weak greenhouse effect, a large part of the incoming shortwave radiation reaches the surface. However, only a small amount of this radiation is absorbed by the surface due to the high surface albedo. In case of a stronger greenhouse effect, less shortwave radiation can penetrate through the clouds, but more longwave radiation is emitted toward the surface due to the greenhouse effect of clouds and water vapor. Hence, clouds impact the net shortwave radiation in two opposite directions: The presence of clouds (1) directly decreases the downward shortwave radiation and (2) indirectly decreases the surface albedo, as surface melt is initiated by the enhanced downwelling radiation at the surface. The latter effect implies that the surface albedo (calculated from ERA-Interim reanalysis using the shortwave fluxes: $\alpha = 1 - \frac{SWN}{SWD}$) in spring is significantly lower in years with a strong greenhouse effect (enhanced downwelling longwave radiation at the surface) than in years with a weak greenhouse effect ($r = -0.43$; significant according to a one-tailed t test, $p < 0.05$). These two processes contribute to the net shortwave radiation in opposite direction and may explain the low predictability of SSIC by the LRM using this variable as predictor (Figure 2b). These two counteracting effects are also reflected in the correlations between spring downwelling longwave radiation and net shortwave radiation (Figure 3): Both variables are significantly anticorrelated in early spring (beginning of April) when the net shortwave radiation is largely determined by clouds and water vapor, as the ocean is still largely covered by sea ice and thus has a high albedo. In late spring (May/beginning of June), however, the correlations with the net shortwave radiation become positive, although correlations with the downwelling shortwave radiation are still negative. This can be explained by the second effect mentioned above: After the melt onset the surface albedo is lowered and more shortwave radiation is absorbed by the surface. Thus, melt is amplified due to the ice albedo feedback which is reflected in significant positive correlations between spring longwave radiation and net short wave radiation later during spring and over the summer.

The low performance of the dry-static and latent energy convergence indicates that spring anomalies of these variables do not significantly contribute to SSIC anomalies [cf. *Kapsch et al.*, 2013]. Rather, it appears to be variables indicative of the greenhouse effect that show the largest predictive skills.

The multiple LRMs, comprising two of the aforementioned predictor variables, perform best among the models for the fitting period. For the prediction period, however, none of the LRMs are showing increased prediction skills compared to the simple LRMs that use only one of these variables. This is likely due to statistical overfitting, implying that too many predictor variables are used compared to the amount of available data [*Wilks*, 2006]. Thus, only the LRMs with one predictor variable will be discussed from here on.

It is noteworthy that the magnitude of the SSIC anomalies are larger in the second part of the observation period (see, e.g., Figure 2a), which likely can be attributed to a thinning of the sea ice cover over the

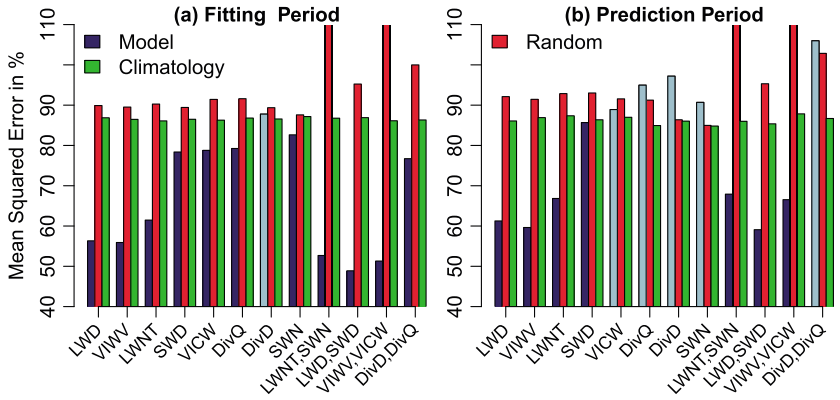

Figure 4. Same as Figure 1 but for the five most negative sea ice anomalies only (1981, 1989, 1990, 1993, and 2007).

considered time period [*Maslanik et al.*, 2007; *Lindsay et al.*, 2008]. As the ice becomes thinner, less energy is needed to melt all ice in a given area. Hence, an anomaly of increased downwelling radiation at the surface in spring induces a larger SSIC anomaly in the second part of the period than in the first part. Therefore, by using a linear regression approach, which, e.g., is fitted over the first 80% of all years, larger errors are expected in the actual prediction period than using, e.g., the last 80% of the period for fitting. To estimate the predictive skill of the LRMs regarding extreme events, the MSE which is more sensitive to outliers than the MAE is calculated for each LRM (Figures 1c and 1d). Except for the LRMs using downwelling longwave radiation and water vapor, all error estimates show a similar or larger magnitude compared to the MSEs of the RC and CP models. Thus, most LRMs are less good in predicting extreme years, e.g., the 1996, 2001, 2007, and 2012 (see also Figure 2a), as compared to other years.

To further investigate the performance regarding extreme years, the error estimates of only the five most extreme negative SSIC anomalies for the fitting and prediction period are presented in Figures 4a and 4b, respectively. The error estimates increase for all of the models (reference LRMs as well as RC and CP models). This indicates that the LRMs are not as good in predicting years with large SSIC anomalies, which is a well-known challenge for seasonal sea ice predictions [*J. Stroeve et al.*, 2014]. However, error estimates for the LRMs based on downwelling longwave radiation, water vapor, and net longwave radiation still outperform the MSEs of RC and CP models. This outlines the importance of the downwelling longwave radiation in spring for the prediction also of the extreme SSIC years. Thus, models that are based on variables closely associated with the greenhouse effect show also predictive skills when it comes to years of extreme SSIC. The multiple linear regression model using downward longwave and shortwave radiation as predictor variables performs the best, as it gives lower error estimates than each of the simple LRMs comprising one of those variables. Note that here the multiple LRM does not seem to overfit. This indicates that these two variables offer different predictive skills that when combined lead to a better performance during extreme SSIC years.

3.2. Implications for Seasonal Sea Ice Prediction

Recent studies show that the trend-independent prediction skills for the September sea ice extent are generally low when it comes to a prediction lead time of several months. In their hindcast, using a coupled atmosphere-ocean sea ice model setup and an initialization of the model in May, *Sigmond et al.* [2013] found a correlation coefficient of less than 0.25 between observed and ensemble mean September ice area. For a similar model setup and the same initialization time but using a perfect model approach, *Day et al.* [2014] found a correlation of about 0.53. Furthermore, *Chevallier et al.* [2013] show that a significant correlation of 0.60 can be obtained for the sea ice extent by focusing specifically on the initialization with realistic initial conditions, in terms of sea ice distribution and thickness as well as the atmospheric variables. To compare to those studies, we calculate the correlation coefficients between modeled and observed SSIC (Figures 1e and 1f). Note that the areas used in the aforementioned publications are comprising the whole Arctic, while we exclude the Greenland, Norwegian, Barents, and Kara Seas (cf. section 2.1).

The correlation coefficients for the prediction period are close to zero for RC and CP models due to their definition and the used Monte Carlo approach. Using our LRMs, we achieve correlation coefficients of 0.5 for the water vapor as predictor variable. This value is almost as high as the coefficient achieved by *Day et al.* [2014]

and *Chevallier et al.* [2013] despite the simplicity of our models and the fact that only atmospheric variables are considered in the LRMs; hence, no information of the sea ice state or oceanic conditions are used. Additionally, neither atmospheric or oceanic processes in summer nor feedback mechanisms due to a melting ice cover are considered in our simple model setup in contrast to the dynamical forecast systems used by *Day et al.* [2014] and *Chevallier et al.* [2013]. The high correlation coefficients between the observed SSIC and the SSIC predicted by the LRMs using water vapor or downwelling longwave radiation underline the importance of the spring atmospheric conditions for the SSIC. The results suggest that the timing and the input of realistic atmospheric initial conditions into the prediction system may play a major role for the predictive skills of a model system. *Schröder et al.* [2014] found that increased melt pond fraction in spring leads to a decreased September sea ice extent. This is consistent with the results presented here, indicating that alterations of the greenhouse effect during spring are important for the SSIC, since an enhanced greenhouse effect leads to increased downwelling longwave radiation toward the surface and ice melt.

4. Summary and Conclusions

Surface downward radiation anomalies during spring show significant predictive skills for the September sea ice extent. This result is obtained using a linear regression technique that takes only the atmospheric conditions in spring (April and May) into account. Hence, neither initial ocean, ice conditions, nor physical processes that affect the sea ice during summer, e.g., ice-ocean or ice-atmosphere feedback processes, are captured in this model approach. However, the prediction skills achieved with this simple approach are comparable to those obtained with fully coupled general circulation models. The results suggest that the spring atmospheric conditions are important for a seasonal prediction of the end-of-summer sea ice extent. Note again that the area used in this study excludes the North Atlantic sector of the Arctic (Greenland, Norwegian, Barents, and Kara Seas), where sea ice concentration is highly affected by the inflow of warm water from the North Atlantic. However, the chosen area includes the major part of the Arctic.

The results show that positive anomalies of spring downwelling longwave radiation and water vapor cause an earlier onset of the sea ice melt in spring, which occurs in the Arctic on average between April and early June [*J. C. Stroeve et al.*, 2014], and thus lead to a lowering of the surface albedo early in the season. Therefore, more downwelling shortwave radiation can be absorbed throughout the summer which is reflected in an amplified melt and a decreased SSIC (Figure 3).

In this study skillful seasonal SSIC predictions are obtained purely based on the described atmospheric processes that take place in the beginning of the melt season. Neither the sea ice state, such as concentration or thickness, nor other processes that act during the summer season (e.g., dynamical wind forcing) are taken into account. This emphasizes the particular importance of the downwelling longwave radiation and water vapor for SSIC predictions and gives evidence that the atmosphere likely plays an essential role for the preconditioning of the SSIC already in spring.

Acknowledgments

We thank two anonymous reviewers for their constructive comments and Bo Christiansen and Richard Bintanja for helpful discussions on the paper. The work is part of the ADSIMNOR (Advanced Simulation of Arctic Climate Change and Impact on Northern Regions) program and funded by the Swedish Research Council FORMAS. The ERA-Interim reanalysis were obtained from the ECMWF data server.

The Editor thanks two anonymous reviewers for their assistance in evaluating this paper.

References

Assessment Arctic Climate Impact (2004), *Impacts of a Warming Arctic*, 139 pp., Cambridge Univ. Press, New York.

Breiman, L., and P. Spector (1992), Submodel selection and evaluation in regression: The X-random case, *Int. Stat. Rev.*, *60*, 291–319.

Cavalieri, D. J., and C. L. Parkinson (2012), Arctic sea ice variability and trends, 1979–2010, *The Cryosphere*, *6*, 881–889, doi:10.5194/tc-6-881-2012.

Chevallier, M., and D. Salas-Mélia (2012), The role of sea ice thickness distribution in the Arctic sea ice potential predictability: A diagnostic approach with a coupled GCM, *J. Clim.*, *25*, 3025–3038, doi:10.1175/JCLI-D-11-00209.1.

Chevallier, M., D. S. Mélia, A. Voldoire, and M. Déqué (2013), Seasonal forecasts of the pan-Arctic sea ice extent using a GCM-based seasonal prediction system, *J. Clim.*, *26*, 6092–6104, doi:10.1175/JCLI-D-12-00612.1.

Day, J. J., S. Tietsche, and E. Hawkins (2014), Pan-Arctic and regional sea ice prediction: Initialisation month dependence, *J. Clim.*, *27*, 4371–4390, doi:10.1175/JCLI-D-13-00614.1.

Dee, D. P., and S. Uppala (2009), Variational bias correction of satellite radiance data in the ERA-Interim reanalysis, *Q. J. R. Meteorol. Soc.*, *135*, 1830–1841, doi:10.1002/qj.493.

Dee, D. P., et al. (2011), The ERA-Interim reanalysis: Configuration and performance of the data assimilation system, *Q. J. R. Meteorol. Soc.*, *137*, 553–597, doi:10.1002/qj.828.

Draper, N. R., and H. Smith (1998), *Applied Regression Analysis*, 3rd ed., Wiley, New York.

Drobot, S. D. (2007), Using remote sensing data to develop seasonal outlooks for Arctic regional sea-ice minimum extent, *Remote Sens. Environ.*, *111*, 136–157, doi:10.1016/j.rse.2007.03.024.

Drobot, S. D., J. A. Maslanik, and C. Fowler (2006), A long-range forecast of Arctic summer sea-ice minimum extent, *Geophys. Res. Lett.*, *33*, L10501, doi:10.1029/2006GL026216.

Eastman, R., and S. G. Warren (2010), Interannual variations of arctic cloud types in relation to sea ice, *J. Clim.*, *23*, 4216–4232.

Eicken, H. (2013), Ocean science: Arctic sea ice needs better forecasts, *Nature*, *497*, 431–433, doi:10.1175/2010JCLI3492.1.

Graversen, R. G., E. Källén, M. Tjernström, and H. Körnich (2007), Atmospheric mass-transport inconsistencies in the ERA-40 reanalysis, *Q. J. R. Meteorol. Soc.*, *133*, 673–680, doi:10.1002/qj.35.

Graversen, R. G., T. Mauritsen, S. Drijfhout, M. Tjernström, and S. Mårtensson (2011), Warm winds from the Pacific caused extensive Arctic sea-ice melt in summer 2007, *Clim. Dyn.*, *36*, 2103–2112, doi:10.1007/s00382-010-0809-z.

Holland, M. M., and C. M. Bitz (2003), Polar amplification of climate change in coupled models, *Clim. Dyn.*, *21*, 221–232, doi:10.1007/s00382-003-0332-6.

Intergovernmental Panel on Climate Change (2013), *Climate Change 2013: The Physical Science Basis. Working Group I Contribution to the Fifth Assessment Report of the Intergovernmental Panel on Climate Change*, edited by T. F. Stocker et al., 1535 pp., Cambridge Univ. Press, Cambridge, U. K., and New York.

Jolliffe, I. T., and D. B. Stephenson (Eds.) (2012), *Forecast Verification: A Practitioner's Guide in Atmospheric Science*, Wiley-Blackwell, Oxford, U. K.

Kapsch, M.-L., R. G. Graversen, and M. Tjernström (2013), Springtime atmospheric energy transport and the control of Arctic summer sea-ice extent, *Nat. Clim. Change*, *3*, 744–748, doi:10.1038/nclimate1884.

Kay, J. E., T. L'Ecuyer, A. Gettelman, G. Stephens, and C. O'Dell (2008), The contribution of cloud and radiation anomalies to the 2007 Arctic sea ice extent minimum, *Geophys. Res. Lett.*, *35*, L08503, doi:10.1029/2008GL033451.

Lindsay, R., M. Wensnahan, A. Schweiger, and J. Zhang (2014), Evaluation of seven different atmospheric reanalysis products in the Arctic, *J. Clim.*, *27*(7), 2588–2606, doi:10.1175/JCLI-D-13-00014.

Lindsay, R. W., J. Zhang, A. Schweiger, M. Steele, and H. Stern (2008), Seasonal predictions of ice extent in the Arctic Ocean, *Geophys. Res. Lett.*, *133*, C02023, doi:10.1029/2007JC004259.

Maksimovich, E., and T. Vihma (2012), The effect of heat fluxes on interannual variability in the spring onset of snow melt in the central Arctic Ocean, *J. Geophys. Res.*, *117*, C07012, doi:10.1029/2011JC007220.

Maslanik, J. A., C. Fowler, J. Stroeve, S. Drobot, J. Zwally, D. Yi, and W. Emery (2007), A younger, thinner Arctic ice cover: Increased potential for rapid, extensive sea-ice loss, *Geophys. Res. Lett.*, *34*, L24501, doi:10.1029/2007GL032043.

Min, S.-K., X. Zhang, F. W. Zwiers, and T. Agnew (2008), Human influence on Arctic sea ice detectable from early 1990s onwards, *Geophys. Res. Lett.*, *35*, L21701, doi:10.1029/2008GL035725.

Ogi, M., and J. M. Wallace (2012), The role of summer surface wind anomalies in the summer Arctic sea ice extent in 2010 and 2011, *Geophys. Res. Lett.*, *39*, 1944–8007, doi:10.1029/2012GL051330.

Schröder, D., D. L. Feltham, D. Flocco, and M. Tsamados (2014), September Arctic sea-ice minimum predicted by spring melt-pond fraction, *Nat. Clim. Change*, *4*, 353–357, doi:10.1038/nclimate2203.

Sedlar, J., and A. Devasthale (2012), Clear-sky thermodynamic and radiative anomalies over a sea ice sensitive region of the Arctic, *J. Geophys. Res.*, *117*, D19111, doi:10.1029/2012JD017754.

Serreze, M. C., and R. G. Barry (2011), Processes and impacts of Arctic amplification: A research synthesis, *Global Planet. Change*, *77*, 85–96, doi:10.1016/j.gloplacha.2011.03.004.

Serreze, M. C., M. M. Holland, and J. Stroeve (2007), Perspectives on the Arctic's shrinking sea-ice cover, *Science*, *315*, 1533–1536, doi:10.1126/science.1139426.

Sigmond, M., J. C. Fyfe, G. M. Flato, V. V. Kharin, and W. J. Merryfield (2013), Seasonal forecast skill of Arctic sea ice area in a dynamical forecast system, *Geophys. Res. Lett.*, *40*, 529–534, doi:10.1002/grl.50129.

Smedsrud, L. H., et al. (2013), The role of the Barents Sea in the Arctic climate system, *Rev. Geophys.*, *51*, 415–449, doi:10.1002/rog.20017.

Stroeve, J., L. C. Hamilton, C. M. Bitz, and E. Blanchard-Wrigglesworth (2014), Predicting September sea ice: Ensemble skill of the SEARCH Sea Ice Outlook 2008Ð2013, *Geophys. Res. Lett.*, *41*, 2411–2418, doi:10.1002/2014GL059388.

Stroeve, J. C., T. Markus, L. Boisvert, J. Miller, and A. Barrett (2014), Changes in Arctic melt season and implications for sea ice loss, *Geophys. Res. Lett.*, *41*, 1216–1225, doi:10.1002/2013GL058951.

Trenberth, K. E. (1991), Climate diagnostics from global analysis: Conservation of mass in ECMWF analysis, *J. Clim.*, *4*, 707–721, doi:10.1175/1520-0442(1991)004<0707:CDFGAC>2.0.CO;2.

Wang, J., J. Zhang, E. Watanabe, M. Ikeda, K. Mizobata, J. E. Walsh, X. Bai, and B. Wu (2009), Is the Dipole Anomaly a major driver to record lows in Arctic summer sea ice extent?, *Geophys. Res. Lett.*, *36*, L05706, doi:10.1029/2008GL036706.

Wang, W., M. Chen, and A. Kumar (2013), Seasonal prediction of Arctic sea ice extent from a coupled dynamical forecast system, *Mon. Weather Rev.*, *141*, 1375–1394, doi:10.1175/MWR-D-12-00057.1.

Wilks, D. S. (2006), *Statistical Methods in the Atmospheric Sciences, Int. Geophys. Ser.*, vol. 91, 2nd ed., 278 pp., Academic Press, Burlington, Mass.

Wu, B., J. E. Overland, and R. D'Arrigo (2012), Anomalous Arctic surface wind patterns and their impacts on September sea ice minima and trend, *Tellus A*, *64*, 18,590, doi:10.3402/tellusa.v64i0.18590.

Zygmuntowska, M., T. Mauritsen, J. Quaas, and L. Kaleschke (2012), Arctic clouds and surface radiation—A critical comparison of satellite retrievals and the ERA-Interim reanalysis, *Atmos. Chem. Phys.*, *12*, 6667–6677, doi:10.5194/acp-12-6667-2012.